

Accepted Manuscript

N-Acyl pyrazoles: effective and tunable inhibitors of serine hydrolases

Katerina Otrubova, Shreyosree Chatterjee, Srijana Ghimire, Benjamin F. Cravatt, Dale L. Boger

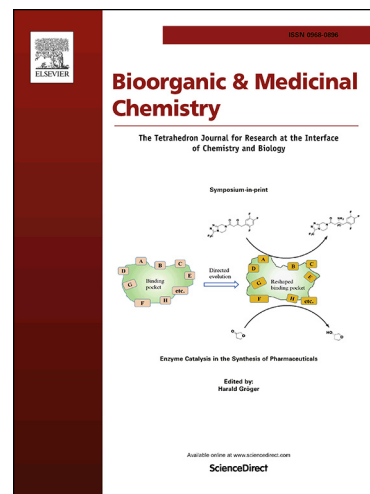
PII: S0968-0896(19)30292-5
DOI: <https://doi.org/10.1016/j.bmc.2019.03.020>
Reference: BMC 14812

To appear in: *Bioorganic & Medicinal Chemistry*

Received Date: 18 February 2019
Revised Date: 8 March 2019
Accepted Date: 8 March 2019

Please cite this article as: Otrubova, K., Chatterjee, S., Ghimire, S., Cravatt, B.F., Boger, D.L., N-Acyl pyrazoles: effective and tunable inhibitors of serine hydrolases, *Bioorganic & Medicinal Chemistry* (2019), doi: <https://doi.org/10.1016/j.bmc.2019.03.020>

This is a PDF file of an unedited manuscript that has been accepted for publication. As a service to our customers we are providing this early version of the manuscript. The manuscript will undergo copyediting, typesetting, and review of the resulting proof before it is published in its final form. Please note that during the production process errors may be discovered which could affect the content, and all legal disclaimers that apply to the journal pertain.



N-Acyl pyrazoles: effective and tunable inhibitors of serine hydrolases

Katerina Otrubova, Shreyosree Chatterjee, Srijana Ghimire, Benjamin F. Cravatt, and Dale L. Boger*

Department of Chemistry and The Skaggs Institute for Chemical Biology, The Scripps Research Institute, 10550 N. Torrey Pines Road, La Jolla, CA 92037, USA

Abstract. A series of N-acyl pyrazoles was examined as candidate serine hydrolase inhibitors in which the active site acylating reactivity and the leaving group ability of the pyrazole could be tuned not only through the nature of the acyl group (reactivity: amide > carbamate > urea), but also through pyrazole C4 substitution with electron-withdrawing or electron-donating substituents. Their impact on enzyme inhibitory activity displayed pronounced effects with the activity improving substantially as one alters both the nature of the reacting carbonyl group (urea > carbamate > amide) and the pyrazole C4 substituent (CN > H > Me). It was further demonstrated that the acyl chain of the N-acyl pyrazole ureas can be used to tailor the potency and selectivity of the inhibitor class to a targeted serine hydrolase. Thus, elaboration of the acyl chain of pyrazole-based ureas provided remarkably potent, irreversible inhibitors of fatty acid amide hydrolase (FAAH, apparent K_i = 100–200 pM), dual inhibitors of FAAH and monoacylglycerol hydrolase (MGLL), or selective inhibitors of MGLL (IC_{50} = 10–20 nM) while simultaneously minimizing off-target activity (e.g., ABHD6 and KIAA1363).

Key words: serine hydrolase inhibitor, N-acyl pyrazole, fatty acid amide hydrolase, monoacylglycerol hydrolase, activity-based protein profiling (ABPP)

*Corresponding author. e-mail address: dale.boger@outlook.com (D L. Boger)

1. Introduction

The endocannabinoids anandamide^{1,2} and 2-arachidonylglycerol (2-AG)^{3,4} are endogenous lipid signaling molecules⁵ that activate cannabinoid (CB1 and CB2) receptors (Figure 1).^{2,6} The characterization and pharmacologic inactivation of the major enzymes that terminate the signaling of anandamide and 2-AG, fatty acid amide hydrolase (FAAH)⁷ and monoacylglycerol lipase (MGLL), respectively,⁸⁻¹¹ have shown that each elevate endocannabinoid signaling and that each affect many

of the same pharmacological processes, including pain and inflammation.¹²⁻¹⁸ Less has been described about simultaneous inhibition of both enzymes, but indications are that it results in more pronounced pharmacological activity.¹⁹ Inhibitors of each enzyme individually or combined could provide therapeutics that replace opioid analgesics for either severe (surgical) or chronic neuropathic pain, avoiding the opioid side effects of dependence, desensitization with chronic dosing, dose-limiting respiratory depression, and constipation that extends hospital stays. Similarly, it is expected such individual or dual enzyme inhibitors could serve as alternatives to medical marijuana or its active constituents in clinical indications where it is presently used, including oncology pain and nausea. Importantly and because they only act on activated signaling pathways, increasing the endogenous concentration of the released signaling molecules only at a site of stimulation, they provide a spatial and temporal pharmacological control not available to direct acting opioid or CB receptor agonists. Herein, we report full details of a study that identified N-acyl pyrazole ureas as candidate serine hydrolase inhibitors and their elaboration to provide selective FAAH inhibitors, dual FAAH/MGLL inhibitors, or selective MGLL inhibitors through modification of distinguishable recognition elements used to target the individual enzyme active sites.

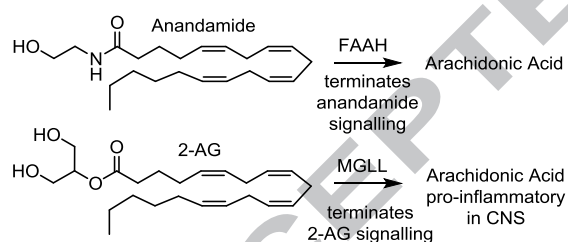


Figure 1. Structures of anandamide and 2-AG.

2. Results and Discussion

In the course of efforts targeting serine hydrolases,^{12,13} we prepared a series of N-acyl pyrazole amides, carbamates and ureas and examined them as candidate inhibitors of the FAAH in order to define their potential utility (Figure 2).²⁰ The compounds were first evaluated in a substrate (oleamide) hydrolysis assay with the pure recombinant rat enzyme (rFAAH) and the results are reported as an apparent K_i that was measured after 3 h preincubation at 25 °C with the enzyme (typically 1 nM, but 0.3 nM for measurement of app $K_i < 2$ nM).²¹ A subsequent gel based activity-based protein profiling

(ABPP) screen was used to assess activity and selectivity,²² which offers the advantage of testing enzymes in their native state and eliminates the need for their recombinant expression, purification, and the development of specific substrate assays. Because the inhibitors are screened against many enzymes in the complex proteome in parallel, their potency and selectivity as well as their performance in cell lysates can be simultaneously evaluated.²³

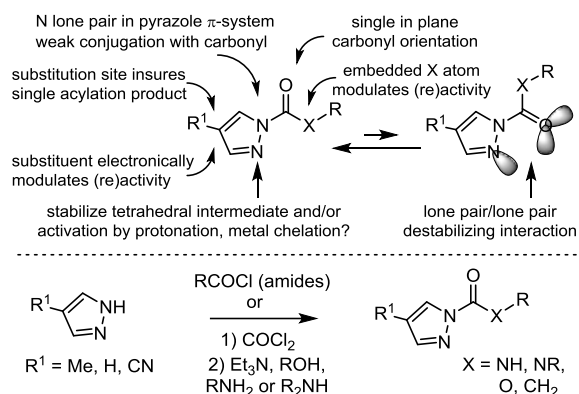


Figure 2. Design and synthesis of candidate N-acyl pyrazole inhibitors.

Precedent for the potential utility of N-acyl pyrazoles was based on the reported behaviour of related azoles (tetrazoles,²⁴ triazoles,²⁵ imidazoles,²⁵ and indazoles²⁵). At the time of our initial communication,²⁰ there were no accounts of detailed or systematic examinations of N-acyl pyrazole ureas or carbamates reacting with or inhibiting serine hydrolases although isolated cases have been disclosed.²⁶ Acyl pyrazoles display an intrinsic modest reactivity toward nucleophilic attack, being less reactive than tetrazoles, triazoles or imidazoles, though they conceivably could be further activated by (enzymatic) protonation or metal chelation. They also represent compounds that contain an activating group potentially capable of formation of a stable (chelated) tetrahedral intermediate.²⁷ The lone pair on the pyrazole nitrogen bound to the carbonyl is not intimately conjugated with the acyl group, as this would diminish the pyrazole aromaticity, making it a potentially good leaving group. Additionally, they are expected to adopt a preferential well-defined acyl orientation with the carbonyl oxygen eclipsed with the in plane pyrazole C5-H and opposite the pyrazole N2 in order to avoid a destabilizing lone pair/lone pair electrostatic interaction (Figure 2). Finally, N-acyl pyrazoles represent a chemotype series in which its acylating reactivity and the leaving group propensity of the pyrazole could be tuned not only by the

nature of the acyl group (reactivity: amide > carbamate > urea), but also through simple symmetrical C4 substitution of the pyrazole with electron-withdrawing or electron-donating substituents (vs unsymmetrical substitution for all other azoles). Notably, electron-withdrawing substituents would be expected to increase the intrinsic leaving group ability of the pyrazole, but would diminish their capabilities for activation by protonation or metal chelation. The importance and impact of these features were first examined and defined with a series N-acyl pyrazoles as inhibitors of FAAH, some of which bear acyl chains known to promote FAAH active site binding (**1–9** and **17–23**) (Figure 3). Each pyrazole inhibitor subset was prepared as an amide, carbamate, or urea and each contained a series of pyrazole substituents (R = Me, H, CN; **a–c**) designed to establish their electronic impact on inhibitor activity (reactivity) and its magnitude. This collection of 69 compounds in itself represents a useful serine hydrolase inhibitor screening sublibrary.²⁰ Several key structural features emerged from their examination. The impact on FAAH inhibitory activity displayed clear and pronounced effects with the activity improving substantially as one alters both the nature of the reacting carbonyl group (urea > carbamate > amide) and the pyrazole C4 substituent (CN > H > Me). Interestingly, the N-acyl pyrazole ureas provided the most potent inhibitors even though they are intrinsically less reactive than the corresponding amides and carbamates, suggesting a unique active site activation for carbamoylation. In contrast, it was the N-acyl pyrazole ureas with the intrinsically more reactive pyrazole leaving group, those bearing the electron-withdrawing C4 substituent (CN), that provided the most potent inhibitors. Additionally, the trends in the impact of the acyl chain were found to follow those expected from observations made with α -ketoheterocycle^{12,13,23} or carbamate/urea¹² inhibitors of FAAH. Thus, the phenalkyl chain inhibitors that contain 5 or 6 atom spacers between the reacting carbonyl and phenyl group^{12d} (**4** and **7** vs **1**) displayed good activity as did those that contain the now characteristic extended and rigidified aryl acyl chains^{12d} (**20–23**), the most potent of which displayed apparent K_i 's of 10–20 nM. Expectedly, the candidate inhibitors with an even shorter phenylalkyl chain were inactive against FAAH (not shown) as were the shorter benzyl (**15–16**), naphthyl (**10–11**), naphthylmethyl (**12–14**) (Figure 3) and related compounds (Figure 4).

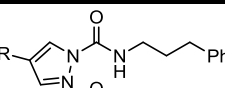
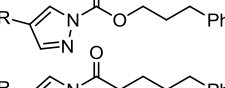
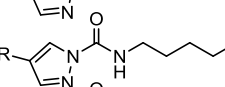
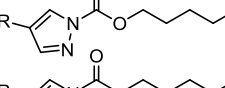
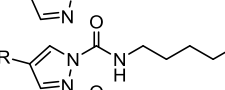
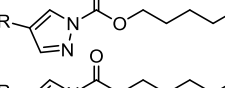
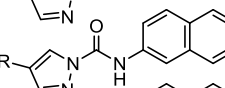
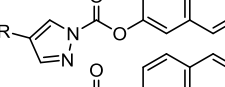
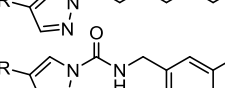
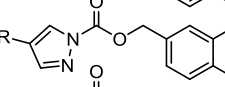
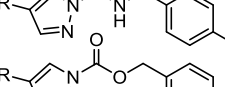
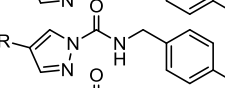
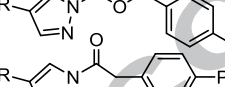
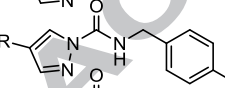
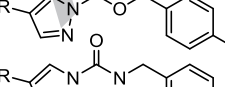
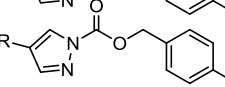
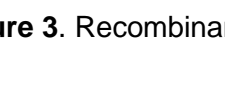


Compound	rFAAH, Apparent K_i (nM) after 3 h preincubation			
	R = Me (a)	H (b)	CN (c)	
1		3000	980	340
2		>5 μ M	>5 μ M	3500
3		>5 μ M	>5 μ M	>5 μ M
4		550	290	18
5		>5 μ M	710	210
6		>5 μ M	>5 μ M	>5 μ M
7		560	280	18
8		>5 μ M	>5 μ M	4200
9		>5 μ M	>5 μ M	>5 μ M
10		>5 μ M	>5 μ M	>5 μ M
11		>5 μ M	>5 μ M	>5 μ M
12		>5 μ M	>5 μ M	>5 μ M
13		>5 μ M	>5 μ M	>5 μ M
14		>5 μ M	>5 μ M	>5 μ M
15		>5 μ M	>5 μ M	>5 μ M
16		>5 μ M	>5 μ M	>5 μ M
17		>5 μ M	>5 μ M	>5 μ M
18		>5 μ M	>5 μ M	>5 μ M
19		>5 μ M	>5 μ M	>5 μ M
20		290	180	9.8
21		580	460	60
22		300	100	17
23		1260	260	145

Figure 3. Recombinant rFAAH inhibition, apparent K_i (25 °C, 3 h preincubation with enzyme, 1 nM).

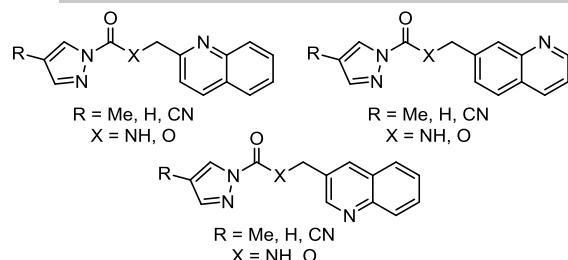


Figure 4. Additional compounds found to be inactive against rFAAH.

The representative members **22a–c** of this series were examined by gel based ABPP in mouse brain proteome as a prelude to the examination of additional inhibitors disclosed later herein (Figure 5). The mouse brain proteome is known to contain FAAH as well as many important off target enzymes observed with earlier classes of FAAH inhibitors, including MGLL and KIAA1363 (also known as arylacetamide deacetylase-like 1 (AADACL1) and neutral cholesterol ester hydrolase 1 (NCEH)). Inhibitors **22a–c** proved to be remarkably selective given their structural simplicity, notably displaying no activity against KIAA1363. By contrast, MGLL was established to be competitively inhibited, and both FAAH and MGLL were inhibited by **22** with near equivalent potencies. Moreover, this near equivalent activity against FAAH and MGLL was observed regardless of the pyrazole substituent, indicating that their impact on intrinsic reactivity and inhibitor potency do not serve to discriminate between the two enzymes. Thus, the same relative potencies of **22a–c** against FAAH in the pure enzyme assay were observed in the gel based assay and their activity against MGLL paralleled these same trends (potency: **22c** > **22b** > **22a**, $R = \text{CN} > \text{H} > \text{Me}$), providing dual balanced inhibitors of the two enzymes.

$R = \text{Me, H, CN}$
 $X = \text{NH, O}$

targets
FAAH = MGLL

22

Compd	ABPP IC ₅₀ (nM) after 1 h preincubation				rFAAH app K _i (nM)
	FAAH	MGLL	ABHD6	KIAA1363	
22a R = Me	1200	1000	nd	>100,000	300
22b R = H	800	900	nd	>100,000	100
22c R = CN	60	100	nd	>100,000	17

nd = not determined

Figure 5. ABPP assays performed after preincubation (1 h, 25 °C) of mouse brain proteome (1 mg/mL) with **22** over a range of inhibitor concentrations. FP-Rhodamine probe (100 nM) was then added and incubated for an additional 20 min.

In many regards, the observation of effective FAAH inhibition with the pyrazole ureas (**1**, **4**, **7**, **20** and **22**) is surprising given the incorporation of monosubstituted carbamides. Typically, FAAH inhibition with urea or carbamate inhibitors is observed with disubstituted carbamide-based ureas or carbamates and seen best with incorporation of rigid, cyclic disubstituted carbamides. With ureas, catalysis of the acylation reaction has been suggested to be derived from an enzyme active site binding-induced conformational change in the urea that diminishes the stabilizing conjugation of the nitrogen lone pair with the carbonyl, activating the urea for nucleophile attack (Figure 6).²⁸ The potential that this binding-induced activation of a urea is FAAH specific has been used to rationalize both the potency and selectivity of other urea-based inhibitors of FAAH.²⁹ As a result, we examined an additional series of 57 N-acyl pyrazole ureas that contain acyclic and cyclic disubstituted carbamides with expectations they may prove to be even more effective inhibitors of FAAH (Figure 6). Each candidate inhibitor set was composed of one of three linkers and one of a series of acyl chains in which each set contained the same three pyrazole substituents (R = Me, H, CN; **a–c**) designed to further establish a leaving group substituent electronic impact on inhibitor activity (reactivity) and its magnitude.

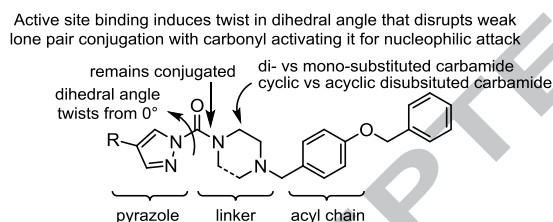


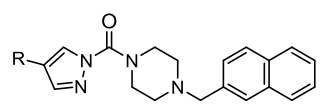
Figure 6. Cyclic and acyclic N-acyl pyrazole ureas containing disubstituted carbamides.

The results of their assessment are summarized in Figure 7 and provided a series of potent FAAH inhibitors. The most potent of these display apparent K_i values of 100–200 pM when substituted with acyl chains we have shown to be especially effective for targeting the FAAH active site.³⁰ Several conclusions are apparent from the results. Even the simple pyrazole ureas **24–27** now display effective inhibition of FAAH, highlighting the productive impact of a fully substituted urea. Moreover, even the more flexible acyclic acyl group found in **27** provided remarkably good inhibition of FAAH. The impact of the C4 pyrazole substituent on FAAH inhibitory activity displayed clear and pronounced effects with the activity improving substantially through each set (R = CN > H > Me).

Compound	rFAAH, Apparent K_i (nM) after 3 h preincubation		
	R = Me (a)	H (b)	CN (c)
24 	>1 μ M	750	80
25 	850	340	55
26 	2900	620	50
27 	710	80	16
<hr/>			
28 	250	180	75
29 	130	9.8	0.16
30 	170	12	0.19
31 	210	9.2	0.10
32 	45	6.1	0.19
33 	100	10	0.16
34 	25	5.8	0.15
<hr/>			
35 	110	9.3	1.0
36 	75	6.3	0.23
37 	230	34	1.5
38 	210	12	0.7
<hr/>			
39 	55	10	2.0
40 	20	5.7	1.2
41 	70	13	3.0
42 	35	6.6	1.3

Figure 7. Recombinant rFAAH inhibition, apparent K_i (25 °C, 3 h preincubation with enzyme at 1 nM for K_i 's > 2 nM and at 0.3 nM for K_i 's < 2 nM). Inhibitors **29–34c** with apparent K_i 's = 0.1–0.2 nM represent stoichiometric irreversible enzyme inhibition under these conditions.

Not only did the electron-withdrawing nitrile group substantially improve activity (CN > H, avg = 25-fold), but even the introduction of a modest electron-donating group diminished activity (H > Me, avg = 8-fold). These distinctions were most pronounced with the rigid, cyclic ureas **28–34** and **35–38**, but still substantial even with the simple (**24–27**) or more flexible acyclic ureas (**39–42**). Although this effect could reflect both an electronic and steric impact of the substituent on the activity, we have shown that FAAH possess a large cytosolic port adjacent to the active site capable of accommodating large substituted heterocycles.³¹ This suggests that the impact is largely or solely due to the electronic properties of the pyrazole C4 substituent. In order to establish whether this truly reflects only the electronic impact of the substituent, an expanded series of substituted pyrazoles was examined in which the electron-withdrawing properties of the C4 substituent was systematically varied without significantly altering its size or polarity (Figure 8). This expanded series exhibited pronounced and incremental increases in potency as the electron-withdrawing properties of the C4 substituent increases (CN > CO₂Me > Br > H > Me), where the change in apparent *K_i* values across the series spans a stunning 10³-fold.



Compound	rFAAH, app <i>K_i</i> (nM) 3 h preincubation
29a R = Me	130
29b H	9.8
29d Br	0.47
29e I	0.29
29f CO ₂ Me	0.36
29c CN	0.16

Figure 8. Impact of pyrazole C4-substituent on inhibition of FAAH.

The time-dependent inhibition of rFAAH was examined with **33a–c** (Figure 9). These three inhibitors are nearly identical in structure, containing the same acyl chain and differing only in the pyrazole C4 substitution. When used in near stoichiometric amounts, all three inhibitors exhibited time-dependent inhibition of rFAAH consistent with irreversible versus reversible competitive inhibition of the enzyme. The intrinsically most reactive of the three inhibitors (**33c**) not only produced the greatest enzyme inhibition at each time point, but also required the shortest time period to reach complete

enzyme inhibition (1 h). Both **33a** and **33b** required a longer and near identical time period to reach maximal enzyme inhibition (ca. 3 h) after which little further decrease in enzyme activity was observed, presumably due to near stoichiometric use of inhibitor and its competitive consumption under the strongly basic conditions of the assay (pH 9), and the intrinsically least reactive of the inhibitors **33a** displayed the smallest degree of enzyme inhibition at each time point. Not only did this confirm time-dependent irreversible enzyme inhibition, but the qualitative results mirror those of the quantitatively measured enzyme inhibition that is reported as apparent K_i . It also established the inhibitor–enzyme preincubation time period (3 h) that we utilized in examination of the inhibitors in the FAAH assay.

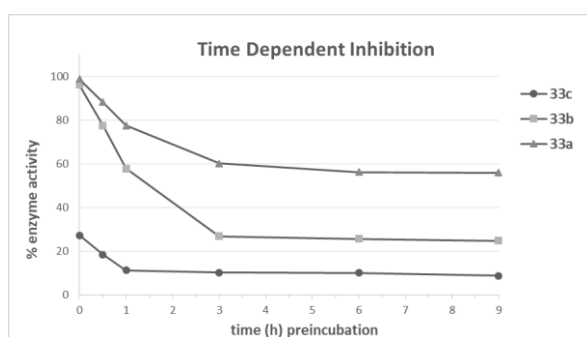


Figure 9. Time-dependent rFAAH inhibition by **33**. rFAAH (2 nM) preincubation (0–9 h, 25 °C, pH 9) with inhibitors **33a–c** (5 nM) followed by measurement of residual enzyme activity.

Two of the potent sets of inhibitors, the three pyrazole ureas bearing the naphthyl tail (**29a–c**) as well as the three containing the 4-benzyloxyphenyl tail (**33a–c**), were each confirmed to be irreversible FAAH inhibitors. Thus, rFAAH was treated with each inhibitor (3 h, 25 °C) at concentrations that resulted in >70% enzyme inhibition. The inhibitor–enzyme mixtures were then subjected to dialysis dilution (4 °C, 18 h) and the residual enzyme activities were measured both before and following dialysis dilution (Figure 10). No recovery of enzyme activity was observed for all six inhibitors after 18 h indicative of irreversible enzyme inhibition by active site carbamoylation of a catalytic serine.

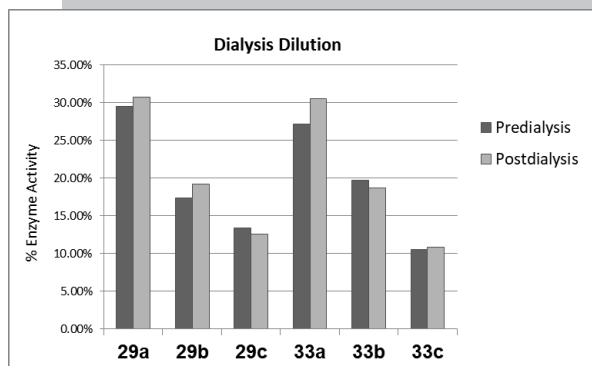
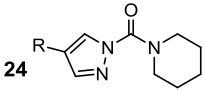


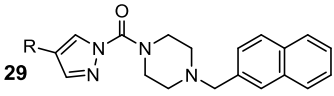
Figure 10. Irreversible rFAAH inhibition by **29** and **33**. rFAAH (2 nM) preincubation (3 h, 25 °C) with inhibitors (**a** at 100 nM, **b** at 50 nM, **c** at 10 nM) and measurement of residual enzyme activity pre and post dialysis dilution (18 h, 4 °C).

Six representative members of this series were examined by gel based ABPP in mouse brain proteome, defining both their potency and intrinsic selectivity in complex proteomes. As highlighted earlier, the mouse brain proteome contains FAAH as well as many of the important off target enzymes observed with earlier classes of FAAH inhibitors, including KIAA1363, MGLL, and ABHD6 ($\alpha\beta$ hydrolase containing domain 6). Like inhibitor **22**, none of the compounds examined displayed activity against KIAA1363. Whereas **24**, lacking an active site targeting acyl tail, inhibited FAAH, MGLL and ABHD6 with near equivalent activities, the inhibitors **29**, **33**, and **37** displayed a divergence in selectivity (Figure 11). Each of these four inhibitors effectively targeted ABHD6, often more effectively than either FAAH or MGLL. MGLL was established to be competitively but less effectively inhibited by **29** and **33**, whereas the further small change in the closely related inhibitor **37** resulted in near complete disruption of MGLL inhibition. This latter compound **37** proved to be quite selective versus MGLL, and displayed dual, often balanced activity against both FAAH and ABHD6. These trends in activity towards the enzymes were observed regardless of the pyrazole substituent, indicating that their impact on intrinsic reactivity and inhibitor potency do not serve to discriminate between these enzymes. Finally, the same relative potencies of **a–c** against rFAAH in the pure enzyme assay were observed in the gel based assay and their relative activity against the competitive enzymes (MGLL and ABHD6) typically also paralleled these same trends (potency: **c** > **b** > **a**, R = CN > H > Me).



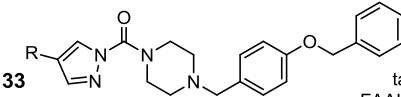
24

Compd	ABPP IC ₅₀ (nM) after 1 h preincubation				rFAAH app K _i (nM)
	FAAH	MGLL	ABHD6	KIAA1363	
24a R = Me	2200	9200	1100	>100,000	>1 μM
24b R = H	1000	6600	5000	>100,000	750
24c R = CN	<10	120	60	>100,000	80



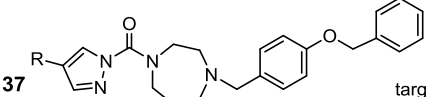
29

Compd	ABPP IC ₅₀ (nM) after 1 h preincubation				rFAAH app K _i (nM)	targets FAAH > MGLL
	FAAH	MGLL	ABHD6	KIAA1363		
29a R = Me	960	920	10	>100,000	130	
29b R = H	90	960	10	>100,000	9.8	
29c R = CN	<10	55	<<10	>100,000	0.16	



33

Compd	ABPP IC ₅₀ (nM) after 1 h preincubation				rFAAH app K _i (nM)	targets FAAH > MGLL
	FAAH	MGLL	ABHD6	KIAA1363		
33a R = Me	650	200	10	>100,000	100	
33b R = H	60	450	220	>100,000	10	
33c R = CN	<<10	<10	<<10	>100,000	0.16	



37

Compd	ABPP IC ₅₀ (nM) after 1 h preincubation				rFAAH app K _i (nM)	targets FAAH >> MGLL
	FAAH	MGLL	ABHD6	KIAA1363		
37a R = Me	560	9,500	9,500	>100,000	230	
37b R = H	450	10,000	960	>100,000	34	
37c R = CN	<<10	10,000	85	>100,000	1.5	

Figure 11. ABPP assays performed after preincubation (1 h, 25 °C) of mouse brain proteome (1 mg/mL) with the each inhibitor over a range of inhibitor concentrations. FP-Rhodamine probe (100 nM) was then added and incubated for an additional 20 min.

By contrast, the pyrazole ureas **41** and **42**, which contained a noncyclic disubstituted carbamide with the same attached groups found in **33** and **37**, were less active in the brain proteome and displayed essentially equal activity against FAAH, MGLL, and ABHD6, displaying little selectivity between the three enzymes (Figure 12). In addition, the same relative potencies of **a–c** against rFAAH in the pure enzyme assay were observed in the gel based assay and their relative activity against the competitive

enzymes (MGLL and ABHD6) smoothly paralleled these same trends (potency: **c** > **b** > **a**, R = CN > H > Me). Cumulatively, these studies demonstrate that N-acyl pyrazole ureas may be used as potent serine hydrolase inhibitors whose (re)activity can be predictably tuned by introduction of pyrazole substituents and whose acyl chain can be tailored to selectively target individual enzymes or more broadly target several closely related enzymes.

41

ABPP IC₅₀ (nM)
after 1 h preincubation

targets
FAAH = MGLL

Compd	FAAH	MGLL	ABHD6	KIAA1363	rFAAH app K _i (nM)
41a R = Me	8700	1200	1200	>100,000	70
41b R = H	510	660	530	>100,000	13
41c R = CN	120	260	320	>100,000	3.0

42

ABPP IC₅₀ (nM)
after 1 h preincubation

targets
FAAH = MGLL

Compd	FAAH	MGLL	ABHD6	KIAA1363	rFAAH app K _i (nM)
42a R = Me	9000	4100	8300	>100,000	35
42b R = H	3000	4600	5500	>100,000	6.6
42c R = CN	190	590	1100	>100,000	1.3

Figure 12. ABPP assays performed after preincubation (1 h, 25 °C) of mouse brain proteome (1 mg/mL) with the each inhibitor over a range of inhibitor concentrations. FP-Rhodamine probe (100 nM) was then added and incubated for an additional 20 min.

In the preceding studies, the candidate inhibitors were outfitted with acyl chains likely to promote binding to MGLL as well as FAAH, and dual balanced FAAH/MGLL inhibitors were discovered (e.g., **41** and **42**) as well as several that displayed greater activity against FAAH (FAAH > MGLL; e.g., **29** and **33**). The series also provided very selective FAAH inhibitors (FAAH >> MGLL, **37**) that can serve as key closely related comparison compounds in the same inhibitor class. However, the series was not designed for and did not define a set of N-acyl pyrazole ureas that act as MGLL selective inhibitors (FAAH < MGLL). Advances in the discovery of selective MGLL inhibitors¹⁵ has been more recent compared to FAAH and even fewer reports have detailed inhibitors with dual FAAH/MGLL inhibition.^{19,32,33} Early on, the irreversible MGLL-selective carbamate-based inhibitors JZL184¹⁶ and

KLM29¹⁷ and the carbamate-based dual FAAH/MGLL inhibitor JZL195 were reported (Figure 13).³³ Although useful, both JZL184 and JZL195 contain a *p*-nitrophenol leaving group that limited in vivo use. To better define the impact of selective MGLL inhibition, continued efforts provided high quality, selective, and in vivo active inhibitors of the enzyme that bear alternative activated carbamates, including the N-hydroxysuccinimide (NHS; e.g. MJN110³⁴) and hexafluoroisopropanol (HFIP; e.g., KLM29¹⁷) derived carbamates. Related inhibitors have since been disclosed.^{35,36} Based on these studies, we examined a series of additional N-acyl pyrazole ureas to illustrate that the acyl chain can be tuned to more selectively target other serine hydrolases, including MGLL.

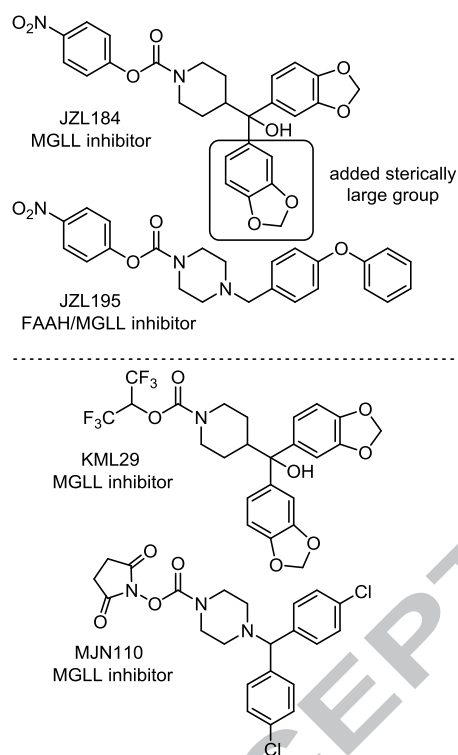
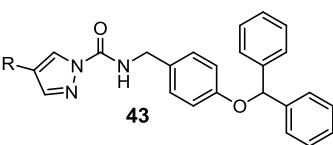


Figure 13. Representative MGLL inhibitors and distinctions with a comparable dual FAAH/MGLL inhibitor.

FAAH and MGLL bind substrates that contain fatty acid chains and often display similar, but not identical acyl chain preferences.³⁷ The distinguishing feature is that MGLL can bind bulkier hydrophobic groups than FAAH (e.g., JZL184 vs JZL195, Figure 13). Since the disclosure of JZL184, a tactic now widely employed relies on the addition of a second, identical and sterically large aryl group to the tail of the acyl chain, disrupting binding to FAAH and maintaining or enhancing binding to MGLL. An additional attractive site to vary is the linker, where a large impact on the FAAH versus MGLL inhibitor activity has also been observed. Consequently, we chose four of the sets of the three related inhibitors (**22**, **41**, **29**,

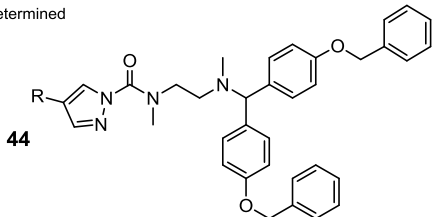
and **33**) with which to probe these effects (**43** vs **22**, **44** vs **41**, **45** vs **29**, and **46** vs **33**). Two of these with the most flexible linker regions composed of either a secondary urea (**43**) or the flexible tertiary urea (**44**) not only abolished nearly all FAAH activity as expected (5,000-fold and 50,000-fold reduction in apparent K_i for **43c** vs **22c** and **44a** vs **41a**, respectively), but also resulted in disrupted activity against all enzymes for which **22** and **41** were effective, including MGLL (e.g., IC_{50} reduced 100-fold for **44c** vs **41c**) (Figure 14).



43

Compd	ABPP IC_{50} (nM) after 1 h preincubation				rFAAH app K_i (nM)
	FAAH	MGLL	ABHD6	KIAA1363	
43a R = Me	>100,000	>100,000	nd	>100,000	220,000
43b R = H	>100,000	>100,000	nd	>100,000	140,000
43c R = CN	>100,000	>100,000	nd	>100,000	80,000

nd = not determined



44

Compd	ABPP IC_{50} (nM) after 1 h preincubation				rFAAH app K_i (nM)
	FAAH	MGLL	ABHD6	KIAA1363	
44a R = Me	>1 mM	>1 mM	>1 mM	>1 mM	140,000
44b R = H	>1 mM	>1 mM	>1 mM	>1 mM	nd
44c R = CN	>1 mM	32,000	>1 mM	>1 mM	nd

nd = not determined

Figure 14. Additional N-acyl pyrazole ureas. ABPP assays performed after preincubation (1 h, 25 °C) of mouse brain proteome (1 mg/mL) with the each inhibitor over a range of inhibitor concentrations. FP-Rhodamine probe (100 nM) was then added and incubated for an additional 20 min.

In contrast, **45** and **46**, which contain the six-membered cyclic tertiary urea, displayed the expected complete disruption of FAAH inhibition and a maintained or enhanced MGLL inhibition relative to **29** and **33**, respectively (Figure 15). Both **45c** and **46c** displayed excellent potency against MGLL (IC_{50} = 8 and 20 nM, respectively). In addition, the competitive or even preferential inhibition of ABHD6 observed with **29** and **33** was also dramatically reduced such that little residual activity was observed with **45** and **46**. For the most potent of the compounds, **45c** and **46c** displayed a 70-fold and >1,000-

fold selectivity for MGLL versus ABHD6. Notably, these distinctions were not as obvious with the less reactive and less active members of the inhibitor sets (R = Me, H), but only apparent with the more reactive members (R = CN).

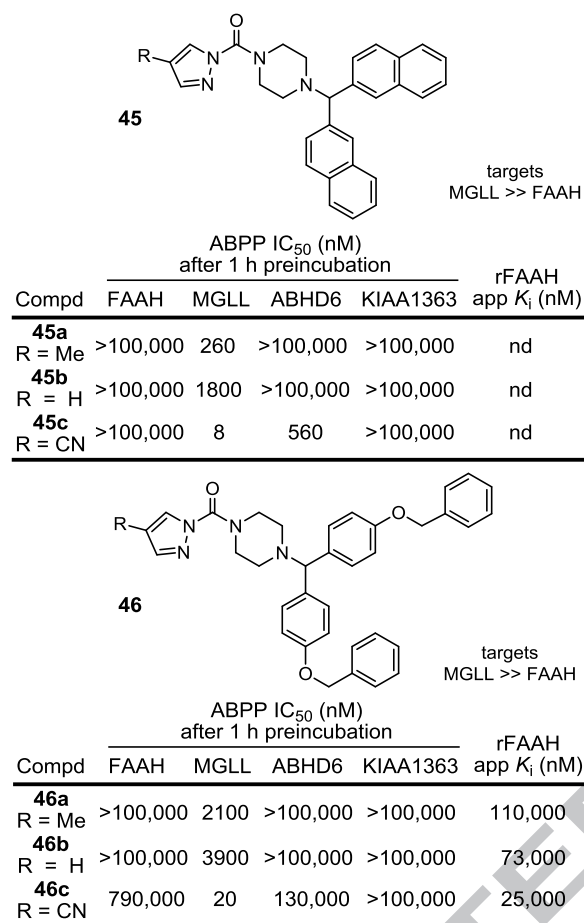


Figure 15. MGLL selective N-acyl pyrazole urea inhibitors. ABPP assays performed after preincubation (1 h, 25 °C) of mouse brain proteome (1 mg/mL) with the each inhibitor over a range of inhibitor concentrations. FP-Rhodamine probe (100 nM) was then added and incubated for an additional 20 min.

Since the pharmacological effects observed with FAAH inhibition require >90% enzyme inhibition while those derived from MGLL inhibition display smoothly increasing effects with an increasing extent of inhibition, the most attractive inhibitors likely will be more potent against FAAH than MGLL. This approach has been validated^{19a,b} using a selective FAAH inhibitor co-administered with a selective MGLL inhibitor. Thus, a high dose of the irreversible FAAH inhibitor PF-3845³⁸ given in combination with a low dose of the irreversible MGLL inhibitor JZL184¹⁶ produced profound increases in brain anandamide levels (>10-fold) but only 2- to 3-fold increases in brain 2-AG levels.¹⁹ This combination produced significantly greater antinociceptive effects than single enzyme inhibition and did

not elicit common cannabimimetic side effects, including catalepsy, hypomotility, hypothermia, and substitution for Δ^9 -THC in a drug-discrimination assay. Moreover, repeated administration of this combination did not lead to tolerance of its antiallodynic actions in the carrageenan assay or to CB1 receptor desensitization. Thus, full FAAH inhibition combined with partial MGLL inhibition reduced neuropathic and inflammatory pain with minimal cannabimimetic effects.¹⁹ Continued exploration of the N-acyl pyrazole ureas could provide an attractive series of closely related inhibitors with which the systematic examination of the effects of the full range of dual inhibition embodied in a single compound could be defined (FAAH > MGLL, balanced FAAH = MGLL, and FAAH < MGLL inhibition potency).

3. Conclusions

A series of N-acyl pyrazoles were examined as candidate serine hydrolase inhibitors and it was shown that active site acylating reactivity and the leaving group ability of the pyrazole could be tuned not only through the nature of the acyl group (reactivity: amide > carbamate > urea), but also through pyrazole C4 substitution with electron-withdrawing or electron-donating substituents. Their impact on FAAH inhibitory activity displayed clear and pronounced effects with the activity improving as one alters both the nature of the reacting carbonyl (urea > carbamate > amide) and the pyrazole C4 substituent (CN > H > Me).⁴² Interestingly, the N-acyl pyrazole ureas provided the most potent inhibitors even though they are intrinsically less reactive than the corresponding amides and carbamates, suggesting a unique active site activation for carbamoylation. In contrast, it was the N-acyl pyrazole ureas with the intrinsically more reactive pyrazole leaving group that provided the most potent inhibitors. It was further shown that the acyl chain of the N-acyl pyrazole ureas can be used to tailor the potency and selectivity of the inhibitor class to a targeted serine hydrolase. Thus, representative modifications of the acyl chain of pyrazole-based ureas provided selective and remarkably potent, irreversible inhibitors of fatty acid amide hydrolase (FAAH, apparent K_i = 100–200 pM), dual inhibitors of FAAH and monoacylglycerol hydrolase (MGLL), or selective potent inhibitors of MGLL (IC_{50} = 10–20 nM).

Finally, and notable in this work, the pyrazole ureas **24a–c** that contain only a simple piperidine carboxamide displayed robust inhibitory activity against FAAH even though they do not contain a

recognition group mimicking the substrate^{27,28} fatty acid amide long chain acyl groups (Figure 7). Rather, they and a small series of pyrazole ureas, including those containing pendant protected secondary amines in the acyl chain, may serve as useful screening compounds used to identify chemotypes selective for inhibition of a subset of serine hydrolases, being more promiscuous across the enzyme class (**25–27**).^{17a} The combined set of **24–27** represent a small, but powerful serine hydrolase screening library (Figure 16).^{39,40} Following detection of a targeted serine hydrolase inhibition, the informative screening leads, which define trends in acyl urea reactivity and the importance of the second attached carbamide (linker), may be divergently modified to improve active site recognition features, simultaneously improving potency and selectivity for a targeted serine hydrolase as demonstrated herein. Thus, their concurrent screening allows the identification of serine hydrolases sensitive to inhibition by the pyrazole ureas, provide initial insights into how reactivity can impact selectivity among the candidate serine hydrolases, define candidate off target enzymes in the class whose activity should be monitored when addressing optimization against a chosen enzyme, and provide superb starting fragments that can be further elaborated to tailor the potency and selectivity of the inhibitor class to a targeted serine hydrolase.⁴³

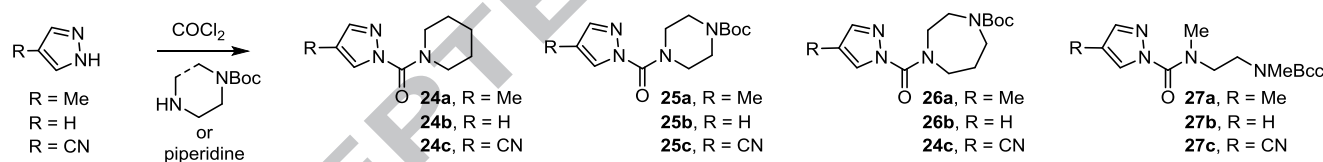


Figure 16. Key members of a serine hydrolase screening library.

4. Experimental

4.1. Chemistry General Methods. All commercial reagents were used without further purification unless otherwise noted. THF was distilled prior to use. All reactions were performed in oven-dried (200 °C) glassware and under an inert atmosphere of anhydrous argon unless otherwise noted. Column chromatography was performed with silica gel 60. TLC was performed on Whatman silica gel (250 μm) F254 glass plates and spots were visualized by UV. PTLC was performed on Whatman silica gel (250 and 500 μm) F254 glass plates. ^1H NMR spectra was recorded on a Bruker 500 or 400 MHz

spectrometer. Chemical shift are measured and reported relative to an internal standard of residual CHCl_3 (δ 7.26 for ^1H). ^1H NMR data are reported as follows: chemical shift (δ), multiplicity (ovlp = overlapping, br = broad, s = singlet, d = doublet, t = triplet, q = quartet, m = multiplet), coupling constant, and integration. High resolution mass spectra was obtained on an Agilent ESI-TOF/MS using Agilent ESI-L low concentration tuning mix as internal high resolution calibration standards. The purity and ESI-LRMS of each tested compound (>95%) were determined on an Agilent 1100 LC/MS instrument using a ZORBAX SB-C18 column (3.5 mm, 4.6 mm \times 50 mm, with a flow rate of 0.75 mL/min and detection at 220 and 253 nm) with a 10–98% acetonitrile/water/0.1% formic acid gradient (two different gradients). Purity analysis and MS characterization may be found in Supporting Information Table S1.

4.1.1. General Procedure for Pyrazole Urea or Carbamate Synthesis. The appropriate pyrazole (1.0 equiv) was treated with phosgene (10 equiv, 20% in toluene) at 0 °C. The reaction mixture was stirred at room temperature for 1 h. The solvent was removed under reduced pressure and the crude carbamoyl chloride was dissolved in anhydrous CH_2Cl_2 (0.5 M). The appropriate amine (1.0 equiv) or alcohol (1 equiv) and Et_3N (1.2 equiv) were dissolved in CH_2Cl_2 (0.5 M) and cooled to 0 °C. The crude carbamoyl chloride was added dropwise and the reaction mixture was stirred at room temperature for 16 h. The mixture was diluted with EtOAc , washed with saturated aqueous NaCl , and dried over Na_2SO_4 . Evaporation under reduced pressure yielded the crude coupling product that was purified by flash chromatography (SiO_2).

4.1.2. General Procedure for Pyrazole Amide Synthesis. The appropriate carboxylic acid (1.0 equiv) was treated with oxalyl chloride (1.1 equiv) in CH_2Cl_2 (0.5 M) at 0 °C. The reaction mixture was stirred at room temperature for 1 h. The solvent was removed under N_2 and the acid chloride (1 equiv) was dissolved in anhydrous CH_2Cl_2 (0.5 M). The appropriate pyrazole (1.0 equiv) was dissolved in CH_2Cl_2 (0.5 M) and cooled to 0 °C. The acid chloride (1 equiv) in CH_2Cl_2 (0.5 M) was added dropwise and the reaction mixture was stirred at room temperature for 3 h. The mixture was diluted with EtOAc , washed with saturated aqueous NaCl , and dried over Na_2SO_4 . Evaporation under reduced pressure yielded the crude product that was purified by flash chromatography (SiO_2).

4.1.3. 1-(4-(4-(Benzyloxy)benzyl)piperazine-1-carbonyl)-1H-pyrazole-4-carbonitrile (**33c**). The title compound was prepared from 1H-pyrazole-4-carbonitrile (8 mg, 0.086 mmol) and 4-(4-benzyloxy)benzylpiperazine (24 mg, 0.086 mmol) by using the general procedure. Flash chromatography (SiO₂, 30% EtOAc–hexanes) afforded **33c** (13 mg, 40%) as a white solid. ¹H NMR (CDCl₃, 400 MHz) δ 8.80 (s, 1H), 8.24 (s, 1H), 7.47 (m, 2H), 7.42 (m, 3H), 7.25 (m, 2H), 7.18 (m, 2H), 5.11 (s, 2H), 3.65 (s, 2H), 3.22 (t, 4H, *J* = 6.7 Hz), 2.54 (t, 4H, *J* = 6.4 Hz). HRMS-ESI-TOF *m/z* 402.1921 ([M+H]⁺, C₂₃H₂₄N₅O₂ requires 402.1930).

4.1.4. 1-(4-(4-(Benzyloxy)benzyl)-1,4-diazepane-1-carbonyl)-1H-pyrazole-4-carbonitrile (**37c**). The title compound was prepared from 1H-pyrazole-4-carbonitrile (10 mg, 0.11 mmol) and 4-(4-(benzyloxy)benzyl)-1,4-diazepane (32 mg, 0.11 mmol) by using the general procedure. Flash chromatography (SiO₂, 40% EtOAc–hexanes) afforded **37c** (13 mg, 28%) as a white solid. ¹H NMR (CDCl₃, 500 MHz) δ 8.80 (s, 1H), 8.28 (s, 1H), 7.47–7.45 (m, 2H), 7.36–7.34 (m, 3H), 7.20–7.18 (m, 2H), 6.85–6.84 (s, 2H), 5.12 (s, 2H), 3.68 (s, 2H), 3.64–3.44 (m, 8H), 1.80 (m, 2H). HRMS-ESI-TOF *m/z* 416.2083 ([M+H]⁺, C₂₄H₂₆N₅O₂ requires 416.2087).

4.2. FAAH Inhibition. ¹⁴C-labeled oleamide was prepared from ¹⁴C-labeled oleic acid. Truncated rat FAAH (rFAAH) was expressed in *E. coli* and purified as described,⁴¹ and the purified recombinant rFAAH was used in the inhibition and reversibility assays. The purity of each tested compound (>95%) was determined on an Agilent 1100 LC/MS instrument using a ZORBAX SB-C18 column (3.5 mm, 4.6 mm × 50 mm, with a flow rate of 0.75 mL/min and detection at 220 and 253 nm) with a 10–98% acetonitrile/water/0.1% formic acid gradient (two different gradients, Supporting Information Table S1).

The inhibition assays were performed as described.^{13,21} The assay was initiated by mixing 1 nM rFAAH (300 pM rFAAH for inhibitors with *K_i* ≤ 1–2 nM) in 500 μL of reaction buffer (125 mM TrisCl, 1 mM EDTA, 0.2% glycerol, 0.02% Triton X-100, 0.4 mM Hepes, pH 9.0) at room temperature in the presence of three different concentrations of inhibitor. After 3 h preincubation at room temperature, The enzyme reaction as initiated by addition of 20 μM of ¹⁴C-labeled oleamide and was terminated by transferring 20 μL of the reaction mixture to 500 μL of 0.1 N HCl at three different time points. The ¹⁴C-

labeled oleamide (substrate) and oleic acid (product) were extracted with EtOAc and analyzed by TLC as detailed.^{13,21} The apparent K_i of the inhibitor was calculated using a Dixon plot.

4.3 Competitive ABPP of inhibitors with FP-rhodamine. Mouse tissues were Dounce-homogenized in PBS buffer (pH 8.0) and membrane proteomes isolated by centrifugation at 4 °C (100,000g, 45 min), washed, resuspended in PBS buffer, and adjusted to a protein concentration of 1 mg/mL. Proteomes were preincubated with inhibitors (10–100,000 nM; DMSO stocks) for 1 h and then treated with FP-rhodamine (100 nM, DMSO stock) at room temperature for 20 min. Reactions were quenched with SDS-PAGE loading buffer, subjected to SDS-PAGE, and visualized in-gel using flatbed fluorescence scanner (MiraBio). Labeled proteins were quantified by measuring integrated band intensities (normalized for volume); control samples (DMSO alone) were considered 100% activity. IC_{50} values ($n = 2-4$) were determined from dose-response curves using Prism software.

4.4. Reversibility of FAAH Inhibition (Dialysis Dilution). The reversibility of FAAH inhibition by **29a–c** and **33a–c** was assessed by dialysis dilution using purified recombinant rat FAAH (rFAAH). The enzyme (2 nM) was placed in 15 mL FAAH assay buffer (125 mM Tris, 1 mM EDTA, 0.2% glycerol, 0.02% Triton X-100, 0.4 mM Hepes, pH 9.0). A 3 mL aliquot of membrane homogenate was used for each sample dialyzed. The dialysis experiment was performed in the pre-dialysis mix at or near the apparent IC_{80} . The final assay inhibitor concentrations used were: **a** at 100 nM, **b** at 50 nM, and **c** at 10 nM. Samples were pre-incubated with the enzyme (2 nM) for 3 h at room temperature (25 °C) before 300 μ L was removed and assayed in triplicate in a FAAH activity assay. The remaining sample (2.7 mL) was injected into a dialysis cassette employing a 10,000 MW cutoff membrane. The mixture was dialyzed against 1 L PBS at 4 °C on a stir plate for 18 h. The post dialysis FAAH activity was assessed by assaying 300 μ L samples taken from the dialysis cassettes in triplicate. FAAH activity is expressed as a percentage of vehicle treated FAAH (DMSO alone).

Acknowledgements

This work was supported by the National Institutes of Health (DA015648, DK114785, DLB; DA037760, BFC). We thank Aleksandar Radakovic and Jelena Momirov for the rFAAH K_i determinations reported in Figures 14 and 15.

Supporting Information

Supplemental data [experimental procedures and characterization data for all tested compounds and table summary of purity analysis of all tested compounds (Table S1)] to this article can be found online at xxxxxx.

Competing interests

D.L.B. and B.F.C. have financial interests in Abide Therapeutics, which has interests in the development of therapeutics derived from inhibition of serine hydrolases.

References

1. Devane WA, Hanus L, Breuer A, Pertwee RG, Stevenson LA, Griffin G, Gibson D, Mandelbaum A, Etinger A, Mechoulam R. Isolation and structure of a brain constituent that binds to the cannabinoid receptor. *Science*. 1992;258:1946–1949.
2. (a) Axelrod J, Felder CC. Cannabinoid receptors and their endogenous agonist, anandamide. *Neurochem Res*. 1998;23:575–581. (b) Di Marzo V, Bisogno T, De Petrocellis L, Melck D, Martin BR. Cannabimimetic fatty acid derivatives: The anandamide family of other endocannabinoids. *Curr Med Chem*. 1999;6:721–744. (c) Martin BR, Mechoulam R, Razdan RK. Discovery and characterization of endogenous cannabinoids. *Life Sci*. 1999;65:573–595.
3. Mechoulam R, Ben-Shabat S, Hanus L, Ligumsky M, Kaminski NE, Schatz AR, Gopher A, Almog S, Martin BR, Compton DR, Pertwee RG, Griffin G, Bayewitch M, Barg J, Vogel Z. Identification of an endogenous 2-monoglyceride, present in canine gut, that binds to cannabinoid receptors. *Biochem Pharmacol*. 1995;50:83–90.
4. Sugiura T, Kondo S, Sukagawa A, Nakane S, Shinoda A, Itoh K, Yamashita A, Waku K. 2-Arachidonoylglycerol: A possible endogenous cannabinoid receptor ligand in brain. *Biochem Biophys Res Commun*. 1995;215:89–97.

5. (a) Ezzili C, Otrubova K, Boger DL. Fatty acid amide signaling molecules. *Bioorg Med Chem Lett*. 2010;20:5959–5968. (b) Boger DL, Henriksen SJ, Cravatt BF. Oleamide: an endogenous sleep-inducing lipid and prototypical member of a new class of biological signaling molecules. *Curr Pharm Design*. 1998;4:303–314.
6. (a) Mackie K. Cannabinoid receptors as therapeutic targets. *Annu Rev Pharmacol Toxicol*. 2006;46:101–122. (b) Cravatt BF, Lichtman AH. The endogenous cannabinoid system and its role in nociceptive behaviour. *J Neurobiol*. 2004;61:148–160.
7. (a) Cravatt BF, Giang DK, Mayfield SP, Boger DL, Lerner RA, Gilula NB. Molecular characterization of an enzyme that degrades neuromodulatory fatty acid amides. *Nature*. 1996;384:83–87. (b) Giang DK, Cravatt BF. Molecular characterization of human and mouse fatty acid amide hydrolases. *Proc Natl Acad Sci USA*. 1997;94:2238–2242.
8. Blankman JL, Simon GM, Cravatt, BF. A comprehensive profile of brain enzymes that hydrolyze the endocannabinoid 2-arachidonoylglycerol. *Chem Biol*. 2007;14:1347–1356.
9. Nomura DK, Hudak CSS, Ward AM, Burston JJ, Issa RS, Fisher KJ, Abood ME, Wiley JL, Lichtman AH, Casida JE. Monoacylglycerol lipase regulates 2-arachidonoylglycerol action and arachidonic acid levels. *Bioorg Med Chem Lett*. 2008;18:5875–5878.
10. Murataeva N, Straiker A, Mackie K. Parsing the players: 2-Arachidonoylglycerol synthesis and degradation in the CNS. *Br J Pharmacol*. 2014;171:1379–1391.
11. Ahn K, McKinney MK, Cravatt BF. Enzymatic pathways that regulate endocannabinoid signaling in the nervous system. *Chem Rev*. 2008;108:1687–1707.
12. (a) Cravatt BF, Lichtman AH. Fatty acid amide hydrolase: An emerging therapeutic target in the endocannabinoid system. *Curr Opin Chem Biol*. 2003;7:469–775. (b) Seierstad M, Breitenbucher JG. Discovery and development of fatty acid amide hydrolase (FAAH) inhibitors. *J Med Chem*. 2008;51:7327–7343. (c) Otrubova K, Ezzili C, Boger DL. The discovery and development of inhibitors of fatty acid amide hydrolase (FAAH). *Bioorg Med Chem Lett*. 2011;21:4674–4685. (d) Otrubova K,

- Boger DL. α -Ketoheterocycle-based inhibitors of fatty acid amide hydrolase. *ACS Chem Neurosci*. 2012;3:340–348.
13. (a) Boger DL, Miyauchi H, Du W, Hardouin C, Fecik RA, Cheng H, Hwang I, Hedrick MP, Leung D, Acevedo O, Guimarães CRW, Jorgensen WL, Cravatt BF. Discovery of a potent, selective, and efficacious class of reversible α -ketoheterocycle inhibitors of fatty acid amide hydrolase as analgesics. *J Med Chem*. 2005;48:1849–1856. (b) Lichtman AH, Leung D, Shelton CC, Saghatelian A, Hardouin C, Boger DL, Cravatt BF. Reversible inhibitors of fatty acid amide hydrolase that promote analgesia: evidence for an unprecedented combination of potency and selectivity. *J Pharmacol Exp Ther*. 2004;311:441–448.
14. Kinsey SG, Long JZ, O'Neal ST, Abdulla RA, Poklis JL, Boger DL, Cravatt BF, Lichtman AH. Blockade of endocannabinoid-degrading enzymes attenuates neuropathic pain. *J Pharmacol Exp Ther*. 2009;330:902–910.
15. (a) Wiener JJM, Cisar JS, Buzard DJ, Weber OD, Grice CA. Development of small molecule inhibitors of monoacylglycerol lipase for the treatment of neurologic diseases. *ACS Med Chem Rev*. 2018;53:463–479. (b) Mulvihill MM, Nomura DK. Therapeutic potential of monoacylglycerol lipase inhibitors. *Life Sci*. 2013;92:492–497. (c) Fowler CJ. Monoacylglycerol lipase - a target for drug development? *Brit J Pharmacol*. 2012;166:1568–1585. (d) Viso A, Cisneros JA, Ortega-Gutierrez S. The medicinal chemistry of agents targeting monoacylglycerol lipase. *Curr Top Med Chem*. 2008;8:231–246.
16. Long JZ, Li W, Booker L, Burston JJ, Kinsey SG, Schlosburg JE, Pavon FJ, Serrano AM, Selley DE, Parsons LH, Lichtman AH, Cravatt BF. Selective blockade of 2-arachidonoylglycerol hydrolysis produces cannabinoid behavioral effects. *Nat Chem Biol*. 2009;5:37–44.
17. Chang JW, Niphakis MJ, Lum, KM, Cognetta AB III, Wang C, Matthews ML, Niessen S, Buczynski MW, Parsons LH, Cravatt BF. Highly selective inhibitors of monoacylglycerol lipase bearing a reactive group that is bioisosteric with endocannabinoid substrates. *Chem Biol*. 2012;19:579–588.

18. Kinsey SG, Long JZ, Cravatt BF, Lichtman AH. Fatty acid amide hydrolase and monoacylglycerol lipase inhibitors produce anti-allodynic effects in mice through distinct cannabinoid receptor mechanisms. *J Pain*. 2010;11:1420–1428.
19. (a) Ghosh S, Kinsey SG, Liu Q, Hrubá L, McMahon LR, Grim TW, Merritt CR, Wise LE, Abdullah RA, Selley DE, Sim-Selley LJ, Cravatt BF, Lichtman AH. Full fatty acid amide hydrolase inhibition combined with partial monoacylglycerol lipase inhibition: Augmented and sustained antinociceptive effects with reduced cannabimimetic side effects in mice. *J Pharmacol Exp Ther*. 2015;354:111–120. (b) Hrubá L, Seillier A, Zaki A, Cravatt BF, Lichtman AH, Giuffrida A, McMahon LR. Simultaneous inhibition of fatty acid amide hydrolase and monoacylglycerol lipase shares discriminative stimulus effects with delta(9)-tetrahydrocannabinol in mice. *J Pharmacol Exp Ther*. 2015;353:261–268. (c) Naidoo V, Karanian DA, Vadivel SK, Locklear JR, Wood JT, Nasr M, Quizon PMP, Graves EE, Shukla V, Makriyannis A, Bahr BA. Equipotent inhibition of fatty acid amide hydrolase and monoacylglycerol lipase - dual targets of the endocannabinoid system to protect against seizure pathology. *Neurotherapeut*. 2012;9:801–813. 86. (d) Long JZ, Nomura DK, Vann RE, Walentiny DM, Booker L, Jin X, Burston JJ, Sim-Selley LJ, Lichtman AH, Wiley JL, Cravatt BF. Dual blockade of FAAH and MAGL identifies behavioral processes regulated by endocannabinoid crosstalk in vivo. *Proc Natl Acad Sci USA*. 2009;106:20270–20275.
20. Otrubova K, Srinivasan V, Boger DL. Discovery libraries targeting the major enzyme classes: The serine hydrolases. *Bioorg Med Chem Lett*. 2014;24:3807–3813.
21. (a) Boger DL, Sato H, Lerner AE, Hedrick MP, Fecik RA, Miyauchi H, Wilkie GD, Austin BJ, Patricelli MP, Cravatt BF. Exceptionally potent inhibitors of fatty acid amide hydrolase: The enzyme responsible for degradation of endogenous oleamide and anandamide. *Proc Natl Acad Sci USA*. 2000;97:5044–5049. (b) Cravatt BF, Prospero-Garcia O, Szuidak G, Henriksen S, Boger DL, Lerner RA. Chemical characterization of a family of brain lipids that induce sleep. *Science*. 1995;268:1506–1509. (c) Cravatt BF, Lerner RA, Boger DL. Structure determination of an endogenous sleep-inducing lipid, cis-9-octadecenoamide (oleamide): a synthetic approach to the chemical analysis of trace quantities of a

natural product. *J Am Chem Soc.* 1996;118:580–590. (d) Patterson JE, Ollmann IR, Cravatt BF, Boger DL, Wong CH, Lerner RA. Inhibition of oleamide hydrolase catalyzed hydrolysis of the endogenous sleep-inducing lipid: cis-9-octadecenamide. *J Am Chem Soc.* 1996;118:5938–5945. (e) Lerner RA, Siuzdak G, Prospero-Garcia O, Hendriksen SJ, Boger DL, Cravatt BF. Cerebrodiene: a brain lipid isolated from sleep-deprived cats. *Proc Natl Acad Sci USA.* 1994;91:9505–9508.

22. (a) Liu Y, Patricelli MP, Cravatt BF. Activity-based protein profiling: The serine hydrolases. *Proc Natl Acad Sci USA.* 1999;96:14694–14699. (b) Kidd D, Liu Y, Cravatt BF. Profiling serine hydrolase activities in complex proteomes. *Biochemistry.* 2001;40:4405–4015. (c) Evans MJ, Cravatt BF. Mechanism-based profiling of enzyme families. *Chem Rev.* 2006;106:3279–3301. (d) Li W, Blankman JL, Cravatt BF. A functional proteomic strategy to discover inhibitors for uncharacterized hydrolases. *J Am Chem Soc.* 2007;129:9594–9595.

23. (a) Leung D, Hardouin C, Boger DL, Cravatt BF. Discovering potent and selective reversible inhibitors of enzymes in complex proteomes. *Nat Biotechnol.* 2003;21:687–691. (b) Leung D, Du W, Hardouin C, Cheng H, Hwang I, Cravatt BF, Boger DL. Discovery of an exceptionally potent and selective class of fatty acid amide hydrolase inhibitors enlisting proteome-wide selectivity screening: Concurrent optimization of enzyme inhibitor potency and selectivity. *Bioorg Med Chem Lett.* 2005;15:1423–1428. (c) Hoover HS, Blankman JL, Niessen S, Cravatt BF. Selectivity of inhibitors of endocannabinoid biosynthesis evaluated by activity-based protein profiling. *Bioorg Med Chem Lett.* 2008;18:5838–5841.

24. (a) Moore SA, Nomikos GG, Dickason–Chesterfield AK, Sohober DA, Schaus JM, Ying BP, Xu YC, Phebus L, Simmons RM, Li D, Iyengar S, Felder CC. Identification of a high-affinity binding site involved in the transport of endocannabinoids. *Proc Natl Acad Sci USA.* 2005;102:17852–17857. (b) Alexander JP, Cravatt BF. The putative endocannabinoid transport blocker LY2183240 is a potent inhibitor of FAAH and several other brain serine hydrolases. *J Am Chem Soc.* 2006;128:9699–9704. (c) Ortar G, Morera E, De Petrocellis L, Ligresti A, Moriello AS, Morera L, Nalli M, Ragno R, Pirolli A, Di Marzo V.

Biaryl tetrazolyl ureas as inhibitors of endocannabinoid metabolism: Modulation at the N-portion and distal phenyl ring. *Eur J Med Chem.* 2013;63:118–132.

25. (a) Ebdrup S, Sorensen LG, Olsen OH, Jacobsen P. Synthesis and structure–activity relationship for a novel class of potent and selective carbamoyl-triazole based inhibitors of hormone sensitive lipase. *J Med Chem.* 2004;47:400–410. (b) Adibekian A, Martin BR, Wang C, Hsu KL, Bachovchin DA, Niessen S, Hoover H, Cravatt BF. Click-generated triazole ureas as ultrapotent in vivo-active serine hydrolase inhibitors. *Nat Chem Biol.* 2011;7:469–478. (c) Morera L, Labar G, Ortar G, Lambert DM. Development and characterization of endocannabinoid hydrolases FAAH and MAGL inhibitors bearing a benzotriazol-1-yl carboxamide scaffold. *Bioorg Med Chem.* 2012;20:6260–6275. (d) Aaltonen N, Savinainen JR, Ribas CR, Ronkko J, Kuusisto A, Korhonen J, Navia-Paldanius D, Hayrinen J, Takabe P, Kasnanen H, Panssar T, Laitinen T, Lehtonen M, Pasonen-Seppanen S, Poso A, Nevalainen T, Laitinen JT. Piperazine and piperidine triazole ureas as ultrapotent and highly selective inhibitors of monoacylglycerol lipase. *Chem Biol.* 2013;20:379–390. (e) Crocetti L, Schepetkin IA, Cilibrizzi A, Graziano A, Vergelli C, Giomi D, Khlebnikov AI, Quinn MT, Giovannoni MP. Optimization of N-benzoylindazole derivatives as inhibitors of human neutrophil elastase. *J Med Chem.* 2013;56:6259–6272. (f) Hsu KL, Tsuboi K, Whitby LR, Speers AE, Pugh H, Inloes J, Cravatt BF. Development and optimization of piperidyl-1,2,3-triazole ureas as selective chemical probes of endocannabinoid biosynthesis. *J Med Chem.* 2013;56:8257–8269. (g) Hsu KL, Tsuboi K, Chang JW, Whitby LR, Speers AE, Pugh H, Cravatt BF. Discovery and optimization of piperidyl-1,2,3-triazole ureas as potent, selective, and in vivo-active inhibitors of alpha/beta-hydrolase domain containing 6 (ABHD6). *J Med Chem.* 2013;56:8270–8279. (h) Patel JZ, Ahenkorah S, Vaara M, Staszewski M, Adams Y, Laitinen T, Navia-Paldanius D, Parkkari T, Savinainen JR, Walczynski K, Laitinen JT, Nevalainen TJ. Loratadine analogues as MAGL inhibitors. *Bioorg Med Chem Lett.* 2015;25:1436–1442. (i) Brindisi M, Maramai S, Gemma S, Brogi S, Grillo A, Di Cesare Mannelli L, Gabellieri E, Lamponi S, Saponara S, Gorelli B, Tedesco D, Bonfiglio T, Landry C, Jung KM, Armirotti A, Luongo L, Ligresti A, Piscitelli F, Bertucci C, Dehouck MP, Campiani G, Maione S, Ghelardini C, Pittaluga A, Piomelli D, Di Marzo V, Butini S.

Development and pharmacological characterization of selective blockers of 2-arachidonoyl glycerol degradation with efficacy in rodent models of multiple sclerosis and pain. *J Med Chem.* 2016;59:2612–2632.

26. (a) Schepetkin IA, Khlebnikov AI, Quinn MT. N-Benzoylpyrazoles are novel small-molecule inhibitors of human neutrophil elastase. *J Med Chem.* 2007;50:4928–4938. (b) Lone AM, Bachovchin DA, Westwood DB, Speers AE, Spicer TP, Fernandez-Vega V, Chase P, Hodder PS, Rosen H, Cravatt BF, Saghatelian A. A substrate-free activity-based protein profiling screen for the discovery of selective PREPL inhibitors. *J Am Chem Soc.* 2011;133:11665–11674. (c) Blankman JL, Cravatt BF. Chemical probes of endocannabinoid metabolism. *Pharmacol Rev.* 2013;65:849–871.

27. Evans DA, Borg G, Scheidt KA. Remarkably stable tetrahedral intermediates: Carbinols from nucleophilic additions to N-acylpyrroles. *Angew Chem Int Ed.* 2002;41:3188–3191.

28. (a) Boger DL, Garbaccio RM. Shape-dependent catalysis: Insights into the source of catalysis for the CC-1065 and duocarmycin DNA alkylation reaction. *Acc Chem Res.* 1999;32:1043–1052. (b) Boger DL, Garbaccio RM. Catalysis of the CC-1065 and duocarmycin DNA alkylation reaction: DNA binding induced conformational change in the agent results in activation. *Bioorg Med Chem.* 1997;5:263–276. (c) Boger DL, Bollinger B, Hertzog DL, Johnson DS, Cai H, Mesini P, Garbaccio RM, Jin Q, Kitos PA. Reversed and sandwiched analogs of duocarmycin SA: Establishment of the origin of the sequence-selective alkylation of DNA and new insights into the source of catalysis. *J Am Chem Soc.* 1997;119:4987–4998. (d) Boger DL, Hertzog DL, Bollinger B, Johnson DS, Cai H, Goldberg J, Turnbull P. Duocarmycin SA shortened, simplified, and extended agents: A systematic examination of the role of the DNA binding subunit. *J Am Chem Soc.* 1997;119:4977–4986. (e) Wolkenberg SE, Boger DL. Mechanisms of in situ activation for DNA-targeting antitumor agents. *Chem Rev.* 2002;102:2477–2495. (f) Tse WC, Boger DL. Sequence-selective DNA recognition: Natural products and nature's lessons. *Chem Biol.* 2004;11:1607–1617. (g) MacMillan KS, Boger DL. Fundamental relationships between structure, reactivity, and biological activity for the duocarmycins and CC-1065. *J Med Chem.* 2009;52:5771–5780.

29. Ahn K, Johnson DS, Fitzgerald LR, Liimatta M, Arendse A, Stevenson T, Lund ET, Nugent RA, Nomanbhoy TK, Alexander JP, Cravatt BF. Novel mechanistic class of fatty acid amide hydrolase inhibitors with remarkable selectivity. *Biochemistry*. 2007;46:13019–13030.
30. (a) Hardouin C, Kelso MJ, Romero FA, Rayl TJ, Leung D, Hwang I, Cravatt BF, Boger DL. Structure–activity relationships of α -ketooxazole inhibitors of fatty acid amide hydrolase. *J Med Chem*. 2007;50:3359–3368. (b) Romero FA, Du W, Hwang I, Rayl TJ, Kimball FS, Leung D, Hoover HS, Apodaca RL, Breitenbucher JG, Cravatt BF, Boger DL. Potent and selective α -ketoheterocycle-based inhibitors of the anandamide and oleamide catabolizing enzyme, fatty acid amide hydrolase. *J Med Chem*. 2007;50:1058–1068. (c) Kimball FS, Romero FA, Ezzili C, Garfinkle J, Rayl TJ, Hochstatter DG, Hwang I, Boger DL. Optimization of α -ketooxazole inhibitors of fatty acid amide hydrolase. *J Med Chem*. 2008;51:937–947. (d) Garfinkle J, Ezzili C, Rayl TJ, Hochstatter DG, Hwang I, Boger DL. Optimization of the central heterocycle of α -ketoheterocycle inhibitors of fatty acid amide hydrolase. *J Med Chem*. 2008;51:4392–4403. (e) Ezzili C, Mileni M, McGlinckey N, Long JZ, Kinsey SG, Hochstatter DG, Stevens RC, Lichtman AH, Cravatt BF, Bilsky EJ, Boger DL. Reversible competitive α -ketoheterocycle inhibitors of fatty acid amide hydrolase containing additional conformational constraints in the acyl side chain: orally active, long acting analgesics. *J Med Chem*. 2011;54:2805–2822.
31. (a) Mileni M, Garfinkle J, DeMartino JK, Cravatt BF, Boger DL, Stevens RC. Binding and inactivation mechanism of a humanized fatty acid amide hydrolase by α -ketoheterocycle inhibitors revealed from cocrystal structures. *J Am Chem Soc*. 2009;131:10497–10506. (b) Mileni M, Garfinkle J, Kimball FS, Cravatt BF, Stevens RC, Boger DL. X-ray crystallographic analysis of α -ketoheterocycle inhibitors bound to a humanized variant of fatty acid amide hydrolase. *J Med Chem*. 2010;53:230–240. (c) Mileni M, Garfinkle J, Ezzili C, Cravatt BF, Stevens RC, Boger DL. Fluoride-mediated capture of a noncovalent bound state of a reversible covalent enzyme inhibitor: X-ray crystallographic analysis of an exceptionally potent α -ketoheterocycle inhibitor of fatty acid amide hydrolase. *J Am Chem Soc*. 2011;133:4092–4100.

32. (a) Korhonen J, Kuusisto A, van Bruchem J, Patel JZ, Laitinen T, Navia-Paldanius D, Laitinen JT, Savinainen JR, Parkkari T, Nevalainen TJ. Piperazine and piperidine carboxamides and carbamates as inhibitors of fatty acid amide hydrolase (FAAH) and monoacylglycerol lipase (MAGL). *Bioorg Med Chem.* 2014;22:6694–6705. (b) Holtfrerich A, Hanekamp W, Lehr M. (4-Phenoxyphenyl)-tetrazolecarboxamides and related compounds as dual inhibitors of fatty acid amide hydrolase (FAAH) and monoacylglycerol lipase (MAGL). *Eur J Med Chem.* 2013;63:64–75. (c) Cisneros JA, Bjorklund E, Gonzalez-Gil I, Hu Y, Canales A, Medrano FJ, Romero A, Ortega-Gutierrez S, Fowler CJ, Lopez-Rodriguez ML. Structure-activity relationship of a new series of reversible dual monoacylglycerol lipase/fatty acid amide hydrolase inhibitors. *J Med Chem.* 2012;55:824–836.
33. (a) Long JZ, Nomura DK, Vann RE, Walentiny DM, Booker L, Jin X, Burston JJ, Sim-Selley LJ, Lichtman AH, Wiley JL, Cravatt BF. Dual blockade of FAAH and MAGL identifies behavioral processes regulated by endocannabinoid crosstalk in vivo. *Proc Natl Acad Sci. USA.* 2009;106:20270–20275. (b) Anderson WB, Gould MJ, Torres RD, Mitchell VA, Vaughan CW. Actions of the dual FAAH/MAGL inhibitor JZL195 in a murine inflammatory pain model. *Neuropharmacol.* 2014;81:224–230.
34. Niphakis MJ, Cognetta AB 3rd, Chang JW, Buczynski MW, Parsons LH, Byrne F, Burston JJ, Chapman V, Cravatt BF. Evaluation of NHS carbamates as a potent and selective class of endocannabinoid hydrolase inhibitors. *ACS Chem Neurosci.* 2013;4:1322–1332.
35. Butler CR, Beck EM, Harris A, Huang Z, McAllister LA, Am Ende CW, Fennell K, Foley TL, Fonseca K, Hawrylik SJ, Johnson DS, Knafels JD, Mente S, Noell GS, Pandit J, Phillips TB, Piro JR, Rogers BN, Samad TA, Wang J, Wan S, Brodney MA. Azetidine and piperidine carbamates as efficient, covalent inhibitors of monoacylglycerol lipase. *J Med Chem.* 2017;60:9860–9873.
36. (a) Cisar JS, Weber OD, Clapper JR, Blankman JL, Henry CL, Simon GM, Alexander JP, Jones TK, Ezekowitz RAB, O'Neill GP, Grice CA. Identification of ABX-1431, a selective inhibitor of monoacylglycerol lipase and clinical candidate for treatment of neurological disorders. *J Med Chem.* 2018;61:9062–9084. (b) McAllister LA, Butler CR, Mente S, O'Neil SV, Fonseca KR, Piro JR, Cianfroga JA, Foley TL, Gilbert AM, Harris AR, Helal CK, Johnson DS, Montgomery JI, Nason DM,

Noell S, Pandit J, Rogers BN, Samad TA, Shaffer CL, da Silva RG, Uccello DP, Webb D, Brodney MA.

Discovery of trifluoromethyl glycol carbamates as potent and selective covalent monoacylglycerol lipase (MAGL) inhibitors for treatment of neuroinflammation. *J Med Chem*. 2018;61:3008–3026.

37. Boger DL, Fecik RA, Patterson JE, Miyauchi H, Patricelli MP, Cravatt BF. Fatty acid amide hydrolase substrate specificity. *Bioorg Med Chem Lett*. 2000;10:2613–2616.

38. Ahn K, Johnson DS, Mileni M, Beidler D, Long JZ, McKinney MK, Weerapana E, Sadagopan N, Liimatta M, Smith SE, Lazerwith S, Stiff C, Kamtekar S, Bhattacharya K, Zhang Y, Swaney S, Van Becelaere K, Stevens RC, Cravatt BF. Discovery and characterization of a highly selective FAAH inhibitor that reduces inflammatory pain. *Chem Biol*. 2009;16:411–420.

39. Available from MilliporeSigma.

40. N-Boc deprotection of **25a–c** to afford the corresponding free amines also provided inhibitors of FAAH that are only two–three-fold less active (app. K_i of 3400, 770, and 90 nM, respectively).

41. Patricelli MP, Lashuel HA, Giang DK, Kelly JW, Cravatt BF. Comparative characterization of a wild type and transmembrane domain-deleted fatty acid amide hydrolase: Identification of the transmembrane domain as a site for oligomerization. *Biochemistry*. 1998;37:15177–15187.

42. (a) Romero FA, Hwang I, Boger DL. Delineation of a fundamental α -ketoheterocycle substituent effect for use in the design of enzyme inhibitors. *J Am Chem Soc*. 2006;128:14004–14005. (b) DeMartino JK, Garfinkle J, Hochstatter DG, Cravatt BF, Boger DL. Exploration of a fundamental substituent effect of α -ketoheterocycle enzyme inhibitors: potent and selective inhibitors of fatty acid amide hydrolase. *Bioorg Med Chem Lett*. 2008;18:5842–5846.

43. A FAAH inhibitor, BIA 10-2474, recently displayed toxicity in the human clinical trials. This toxicity is not intrinsic to inhibiting the target enzyme FAAH. There is not yet a consensus on how the toxicity arises and even whether it was related to the selectivity of BIA 10-2474 toward other serine hydrolases, its greater in situ versus in vitro activity due to intracellular accumulation, or the trial design that enlisted repeat multiple dosing at levels far above that needed for 100% target engagement and where PK/PD parameters are no longer linear. However, it is worth highlighting that the N-acyl pyrazoles, unlike the

